

Ferromagnetic resonance in Yttrium Iron Garnet

Author: Sara Santamaría Hernández.

*Facultat de Física, Universitat de Barcelona, Diagonal 645, 08028 Barcelona, Spain.**

Advisor: Joan Manel Hernández Ferràs

Abstract: This work presents a study of the ferromagnetic resonance of an Yttrium Iron Garnet sample with thickness of 25 nm. From the experimental data, the values that have been obtained are the gyromagnetic ratio, the saturation magnetization, the magnetic anisotropy and the damping factor for the external magnetic field parallel and perpendicular to the sample surface.

I. INTRODUCTION

Ferromagnetic resonance (FMR) is a method that applies the magnetic resonance (MR) to ferromagnetic materials. MR measures magnetic properties by detecting the precessional motion of the magnetization when this magnetization is oriented by an external static magnetic field. Resonance phenomena occurs when the frequency of an external oscillating field, applied transversely to the magnetic moment of the material, is equal to the precession frequency. This frequency is known as Larmor precession frequency and depends on the magnetic sample, the static magnetic field and the oscillating magnetic field applied. At this frequency, the magnetic moment can absorb the energy of the oscillating magnetic field resulting in a change of its precession. In ferromagnets, the Larmor frequency is about GHz. To produce ferromagnetic resonance it will be used electromagnetic waves (microwaves) that will be sent perpendicularly to the sample. However, this absorbed energy is dissipated in time due to the spin-orbit interaction, the interaction between the spins of material and the spins of the impurities, or the interaction with free electrons. These interactions generate a damping process, that makes spins lose their precession and tend to orientate them in the direction of the magnetic field.

In this work, it has been used a broadband FMR setup to obtain the value of the gyromagnetic ratio, the saturation magnetization, the magnetic anisotropy and the damping factor for a sample of Yttrium Iron Garnet.

II. THEORETICAL FRAMEWORK

To describe the dynamics of the ferromagnetic resonance and several important physical systems, Landau-Lifshitz-Gilbert (LLG) equation is used. In this section, it will be presented a brief derivation of this equation.

In atoms, the magnetic moment $\vec{\mu}$ lies along the same direction as the angular momentum \vec{L} of their orbiting

electrons [1], and is proportional to it as

$$\vec{\mu} = -\gamma \vec{L}$$

This relation is the basis of the Larmor theorem, where $\gamma = \frac{g|e|\hbar}{2m_e} = \frac{g\mu_B}{\hbar}$ is a constant known as the gyromagnetic ratio, g is the Landé factor, e is the elementary charge, m_e is the mass of the electron, μ_B is the Bohr magneton and \hbar is the reduced Planck's constant. Now, if we consider a magnetic moment, $\vec{\mu}$, in a static magnetic field, \vec{B} , the energy, E , of the magnetic moment is given by

$$E = -\vec{\mu} \cdot \vec{B}$$

So the energy is minimized when the magnetic moment lies along the magnetic field. It will exist a torque \vec{G} on the magnetic moment given by

$$\vec{G} = \vec{\mu} \times \vec{B} \quad (1)$$

which would try to align the magnetic moment along the direction of the magnetic field. Dividing by the volume we obtain the same expression in terms of magnetization, $\vec{M} = \frac{\vec{\mu}}{V}$. However, since the magnetic moment is associated with the angular momentum \vec{L} , and because torque is equal to rate of change of angular momentum, Eq.(1) can be rewritten as

$$\frac{d\vec{M}}{dt} = -\gamma(\vec{M} \times \vec{B}) \quad (2)$$

So the torque will cause the magnetization to precess around the magnetic field, as it can be seen in Fig. 1 (a), at the Larmor frequency

$$\omega = \gamma B \quad (3)$$

that can be obtained solving Eq.(2). This frequency in Eq.(3) considers a spherical symmetry, but we can apply different conditions depending on the symmetry of our system. Considering a system with the static magnetic field applied tangentially to the ferromagnetic sample surface, and taking into account the demagnetizing field, the expression is written as:

$$\omega = \frac{\gamma}{2\pi} \sqrt{B_i(B_i + \mu_0 M_S)} \quad (4)$$

*Electronic address: santamariahernandez.sara@gmail.com

If our sample is perpendicular to the magnetic field, the resonant frequency is:

$$\omega = \frac{\gamma}{2\pi}(B_i - \mu_0 M_S) \quad (5)$$

where M_S is the saturation magnetization and B_i is composed by the external magnetic field, B_{ext} , and an effective magnetic field associated to the anisotropies of the sample, B_{anis} .

As it has been mentioned in the introduction, dissipative interactions have been not considered in Eq.(2). So these interactions add a new magnetic moment force in the equation of motion of the magnetization, represented in Fig. 1 (b). These terms were introduced first by Landau and Lifshitz (1935) and later by Gilbert (1955). The result is the Landau-Lifshitz-Gilbert (LLG) [2] equation:

$$\frac{d\vec{M}}{dt} = -\gamma(\vec{M} \times \vec{B}) + \frac{\alpha}{M_S}(\vec{M} \times \frac{d\vec{M}}{dt}) \quad (6)$$

Where α is the dimensionless damping parameter.

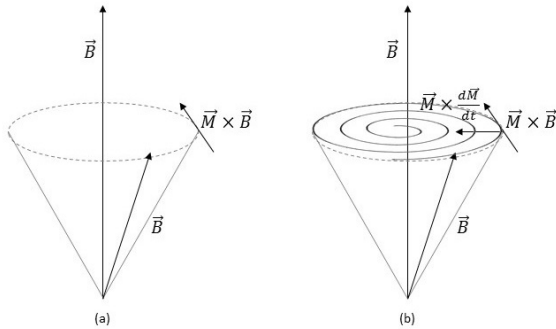


FIG. 1: Evolution of magnetization (a) in the presence of a magnetic field and (b) when damping is included.

This new term is responsible for the absorption peak, which has a bandwidth or linewidth ΔB , in terms of magnetic field. In the framework of the LLG model for damping, the linewidth [3] depends linearly on the product of the resonant frequency and the damping parameter. The measured linewidth can be written in terms of frequency [2] as:

$$\Delta B = \Delta B_0 + 4\pi\alpha \frac{\omega}{\gamma} \quad (7)$$

where ΔB_0 contains all the extrinsic contributions, like inhomogeneities. Thus, the damping parameter α can be obtained from the slope of the linewidth as a function of microwave frequency plot.

Using ferromagnetic resonance, we can obtain γ and M_S by fitting the experimental data of resonant frequency to a function like Eq.(4) or Eq.(5) depending on the geometry of our system, and α to a function like Eq.(7).

III. EXPERIMENTAL PROCESS

To study the ferromagnetic resonance, we should apply an external static magnetic field, B_{ext} , and measure the energy absorbed by the sample. To realize the experiment, we have used the following experimental setup: a power supply, an electromagnet, a Hall probe, a VNA vector network analyzer, a coplanar waveguide, the ferromagnetic sample that wants to be studied and a computer to save and analyze data collection. We can observe a drawing of the experimental setup in Fig. 2.

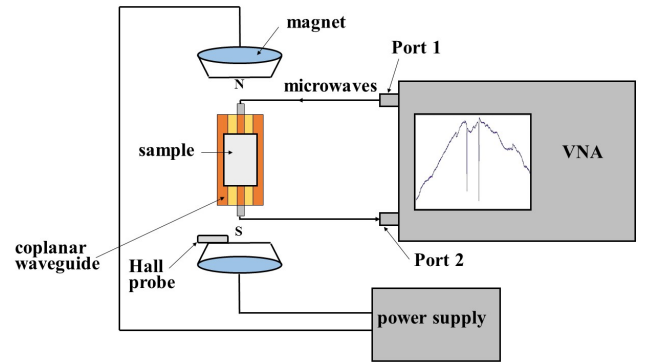


FIG. 2: Experimental setup.

The power supply generates the electric current to create the external static magnetic field inside the magnet. The Hall probe measures the transverse voltage produced that we can convert in magnetic field with a linear equation.

The VNA is a vector network analyzer used in magnetic experiments with microwaves frequencies. It has two ports: one that sends microwaves to the sample and the other that receives the microwave intensity after crossing the ferromagnet.

The coplanar waveguide, composed by a dielectric substrate, propagates the microwaves from the source to the sample. It has one face coated by three metal strips. The lateral tracks have ground connection and depending on the width of the central strip and the separation between this and the others, the electrical parameters could be changed.

The ferromagnetic sample used in this experiment is Yttrium Iron Garnet, commonly known as YIG, that is an insulator magnet with composition $Y_3Fe_5O_{12}$. This ferrimagnetic material has caused a great interest since its discovery due to its properties, which make it very appropriate for magnetic studies. The magnetic properties of YIG [4] come from the ferromagnetic interaction between iron ions with same coordination and the antiferromagnetic interactions between ions with different coordination. Two properties that should be noted are that YIG has the lowest known spin-wave damping factor and that this material presents a very small linewidth in a ferromagnetic resonance experiment. In addition, another important property to our experimental process is

that the anisotropy field of YIG is very small, so the magnetic field of equations (4) and (5) will be only the external magnetic field, in a first approximation.

In the experimental procedure, the sample to be studied (YIG) is placed on the central conductor of the coplanar waveguide, in the center of the electromagnet. Then the VNA sends and receives microwaves with a frequency sweep at several external magnetic fields created by the magnets. The computer collects the data of the hall voltage, the frequency and the intensity S_{21} , that corresponds to the ratio of the received power in port 2 and the input power in port 1 of VNA. This sweeps of frequency and magnetic field are controlled with a LabView program with the computer.

IV. EXPERIMENTAL RESULTS

The results exposed in this section are for two different geometries: external magnetic field parallel (0 degrees) and perpendicular (90 degrees) to the sample surface of YIG.

For the first one, a frequency sweep of 40 points has been done from 500 MHz to 20 GHz for every magnetic field. Using steps of 0.001 T, this magnetic field took values between -0.6 T and 0.6 T. For the external static magnetic field perpendicular to the sample surface, the frequency sweep was the same, but the magnetic field range was from -0.8 T to 0.8 T with steps of 0.0025 T.

First of all, the data collected of Hall voltage has to be converted to magnetic field with a linear equation. By plotting the frequency ω versus magnetic field B_{ext} and the rate of power S_{21} , it can be observed two branches that correspond to the resonance frequencies at positive and negative magnetic fields, as it can be seen in Fig. 3 for the magnetic field parallel to the sample surface. It has been obtained a similar plot applying the magnetic field at 90 degrees, but in this case the branches do not cross the x-axis at zero.

If we make a cut in a certain frequency of Fig. 3, we will obtain a plot like Fig. 4, where we can observe the intensity profile for a frequency of 3.5 GHz. The peaks correspond to the ferromagnetic resonance phenomena.

To verify that the experimental data follows the theory, we can select one of the resonance peaks to study how its position (resonant field) changes for different frequencies. A plot of ω versus the resonant field B_{ext} should be represented to fit the experimental data to a suitable function.

From the Fig. 5, that corresponds to B_{ext} in plane, it can be seen that the resonances seem to follow a law that goes like $\omega \propto B_{ext}^{1/2}$. We can rewrite Eq.(4) from theory as

$$\frac{\omega^2}{B_{ext}} = \gamma_e^2 (B_{ext} + \mu_0 M_S) \quad (8)$$

where $\gamma_e = \frac{\gamma}{2\pi}$. By fitting $\frac{\omega^2}{B_{ext}}(B_{ext})$ to a linear function, it can be obtained the value of $\mu_0 M_S$ and γ_e . However,

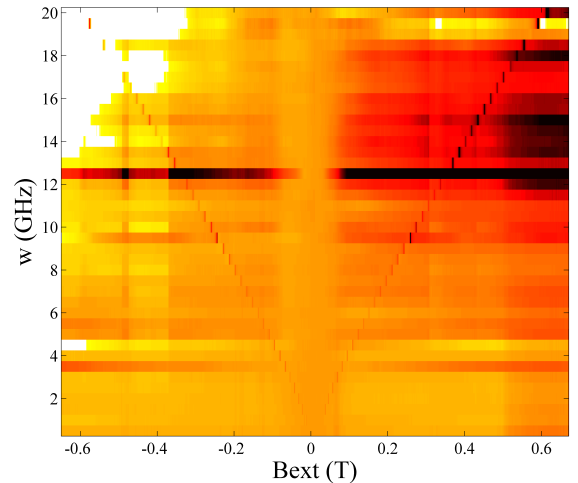


FIG. 3: Frequency ω vs. magnetic field (T) and microwave transmission S_{21} in color scale for the magnetic field parallel to the sample surface.

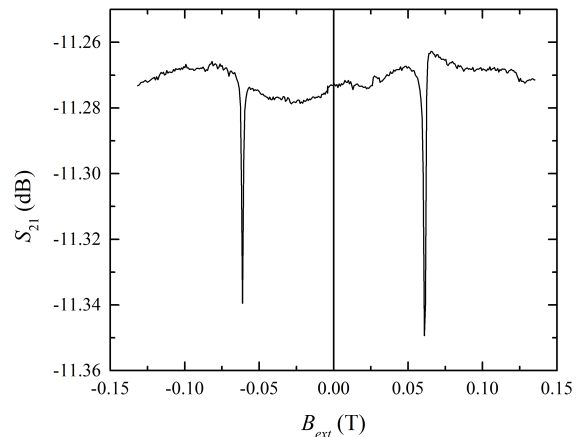


FIG. 4: Intensity profile S_{21} vs. magnetic field B_{ext} for a frequency of 3.5 GHz for the magnetic field parallel to the sample surface.

the result of this plot is not a perfect linear function, due to the magnetic anisotropy field contribution. As it has been mentioned before, the magnetic field is composed by the external magnetic field and an effective magnetic field. In a first approximation we can suppose that the effective magnetic field is negligible, but it is not true because we can not do a perfect linear fit of our plot. So the data points have to be adjusted by adding a new term in Eq.(8) that can be rewritten as:

$$\frac{\omega^2}{B_{ext} + B_{anis}^{\parallel}} = \gamma_e^2 (B_{ext} + B_{anis}^{\parallel} + \mu_0 M_S) \quad (9)$$

where B_{ext} is the applied static magnetic field, which is

the data collected, and B_{anis}^{\parallel} is the magnetic anisotropy field that in this case is $B_{anis}^{\parallel} = 0.0048 \pm 0.0002$ T. This is the value of magnetic anisotropy that has to be added to our static magnetic field to fit the data points to a linear function. The result of this fit, that can be seen in Fig 6, is $\mu_0 M_S = 0.1836 \pm 0.0012$ T and $\gamma_e = 27.27 \pm 0.07 \frac{\text{GHz}}{\text{T}}$.

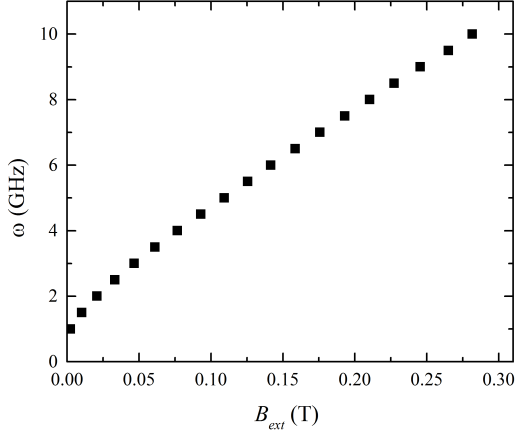


FIG. 5: Frequency ω vs. resonant magnetic field B_{ext} , for magnetic field parallel to the sample surface.

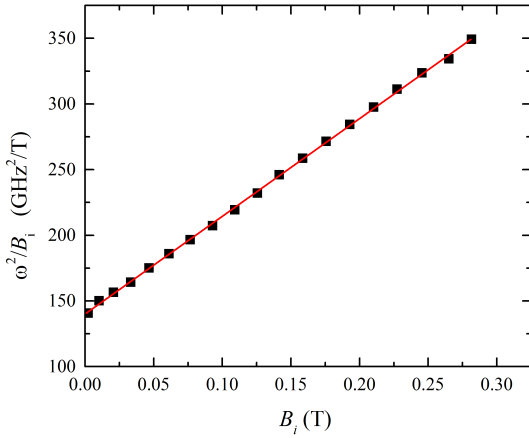


FIG. 6: $\frac{\omega^2}{B_i^2}$ vs. B_i and fit of datapoints, for magnetic field parallel to the sample surface.

The same procedure should be done for the magnetic field out of plane. In this case, the resonances seem to follow a law that goes like $\omega \propto B_{ext}$. By fitting the experimental data of $\omega(B_{ext})$ to a linear function, it can be obtained the value of γ_e and $\mu_0 M_S + B_{anis}$, comparing with Eq.(5). The saturation magnetization has to be constant, so in this case it has been used the value of $\mu_0 M_S$ obtained for magnetic field in plane to find the magnetic anisotropy field in this direction. This fit can

be seen in Fig. 7, and the values obtained are $\gamma_e = 26.34 \pm 0.08 \frac{\text{GHz}}{\text{T}}$ and $\mu_0 M_S - B_{anis}^{\perp} = -0.2004 \pm 0.0007$ T. With $\mu_0 M_S = 0.1836 \pm 0.0017$ T, we obtain $B_{anis}^{\perp} = -0.0168 \pm 0.0005$ T.

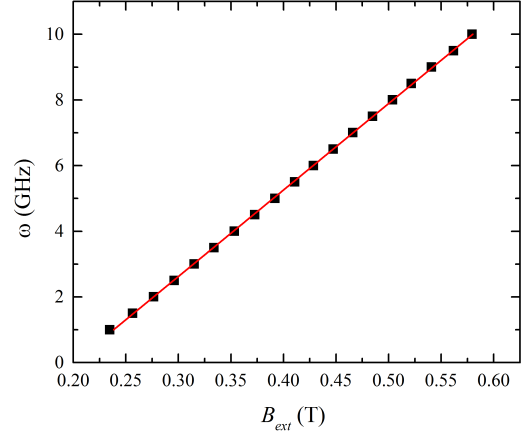


FIG. 7: Frequency ω vs. resonant magnetic field B_{ext} and fit of datapoints, for the magnetic field perpendicular to the sample surface.

In addition, we can find the damping parameter from the experimental data. The resonance peaks can be fitted by a Lorentzian equation to find the Full Width at Half Maximum (FWHM), that corresponds [3] to the linewidth ΔB . Then, by plotting ΔB versus ω the damping parameter α can be obtained computing the slope of data points, according to Eq.(7) from theoretical framework. In Fig. 8 we can observe the fit of the experimental data for the magnetic field parallel to the sample surface. These points are very disperse due to the approximations made to calculate the FWHM. To calculate the value of the damping parameter from the slope, it has been used the value of the gyromagnetic ratio obtained previously, that is $\gamma_e = 27.27 \pm 0.07 \frac{\text{GHz}}{\text{T}}$. The value found was $\alpha = 0.00101 \pm 0.00006$.

We should follow the same procedure to find the damping parameter with the magnetic field perpendicular to the sample surface. We can observe the fit of datapoints in Fig. 9. In this case, the value used of gyromagnetic ratio is $\gamma_e = 26.34 \pm 0.08 \frac{\text{GHz}}{\text{T}}$ and the value of damping parameter obtained is $\alpha = 0.00091 \pm 0.00008$.

The values obtained could be considered correct for two reasons: The first one is that the values of damping for the sample parallel and perpendicular to the external magnetic field are practically the same. This is a good indicator because damping is a constant parameter of each material. And the second one is that YIG has a damping factor of $10^{-4} - 10^{-5}$, and the value obtained is in this range.

Finally, the mean between these values can be done to affirm that the damping factor of our sample of YIG is $\alpha = 0.00096 \pm 0.00010$.

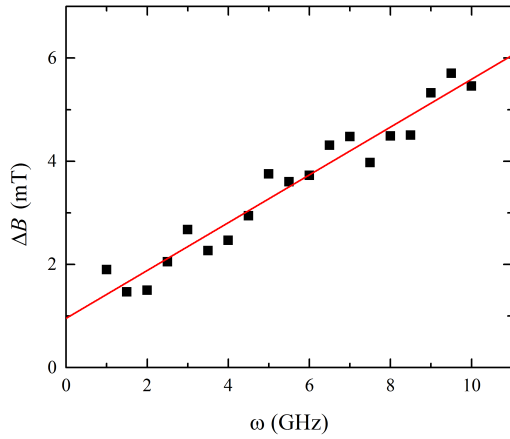


FIG. 8: FWHM ΔB (T) vs. resonant frequency ω (GHz) and fit of datapoints, for the sample tangential to H.

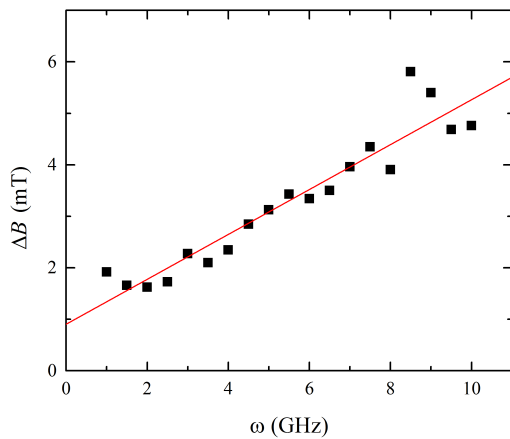


FIG. 9: FWHM ΔB (T) vs. resonant frequency ω (GHz) and fit of datapoints, for the sample perpendicular to H.

V. CONCLUSIONS

In this work it has been characterized a sample of YIG with FMR. The values found in literature for the gyro-

magnetic ratio is $\gamma_e = 28.025 \frac{\text{GHz}}{\text{T}}$, and the saturation magnetization and the damping factor for YIG [5] are $\mu_0 M_S = 0.17 - 0.18 \text{ T}$ and $\alpha = 10^{-4} - 10^{-5}$ respectively. The values obtained for the gyromagnetic ratio are: $\gamma_e = 27.27 \pm 0.07 \frac{\text{GHz}}{\text{T}}$ for the sample parallel to external magnetic field and $\gamma_e = 26.34 \pm 0.08 \frac{\text{GHz}}{\text{T}}$ for the sample perpendicular to it. These values have a significant difference with the value of literature for the two inclinations of the sample. Probably, this fact is due to the calibration of the Hall sensor which is very delicate.

For saturation magnetization it has been found the value $\mu_0 M_S = 0.1836 \pm 0.0012 \text{ T}$ and it can be considered a correct value for YIG, although it is not between 0.17 and 0.18 T. This value was found by fitting data points of Fig. 6 considering a magnetic anisotropy field of $B_{anis}^{\parallel} = 0.0048 \pm 0.0002 \text{ T}$, with magnetic field in plane. Our points do not describe a perfect linear function, so this value of magnetic anisotropy is not completely exact and affects when the saturation magnetization wants to be found. Considering this saturation magnetization as a correct value, it has been obtained the magnetic anisotropy for the magnetic field out of plane: $B_{anis}^{\perp} = -0.0168 \pm 0.0005 \text{ T}$. Comparing the two values of anisotropy, it can be conclude that exists a preferred orientation: magnetization parallel to the sample surface. The positive sign of B_{anis}^{\parallel} shows that anisotropy wants magnetization to stay in plane. This agrees with the negative sign of B_{anis}^{\perp} , that opposes to the out of plane external magnetic field.

Finally, it has been found that the damping factor is $\alpha = 0.00096 \pm 0.00010$, which can be considered a correct value because it is between limits of the value of the literature.

The results show that broadband FMR could be a good method to characterize the magnetic properties of materials with a correct precision.

Acknowledgments

I would like to thank my advisor Dr. Joan Manel Hernández Ferràs for his guidance and help in this work. Also I want to thank my family and my friends for their support during the realization of this work.

-
- [1] Stephen Blundell, *Magnetism in Condensed Matter*, (Oxford University Press, New York 2001, 13th. ed.).
 - [2] J. Pelzl, R. Meckenstock, D. Spoddig, F. Schreiber, J. Pflaum and Z. Fraai, "Spinorbit-coupling effects on g-value and damping factor of the ferromagnetic resonance in Co and Fe films", *J. Phys.: Condens. Matter* **15** (2003).
 - [3] H. T. Nembach, T. J. Silva, J. M. Shaw, M. L. Schneider, M. J. Carey, S. Maat, and J. R. Childress, "Perpendicular ferromagnetic resonance measurements of damping and

- Landé g factor in sputtered $(\text{Co}_2\text{Mn})_{1-x}\text{Ge}_x$ thin films", *Physical Review B* **84**, 054424 (2011).
- [4] Antonio Fernández Martínez, *Estudi de Materials Magnètics en Microones*, Ph.D thesis (Universitat de Barcelona, 2014).
- [5] S. Klingler, A. Conca, A. V. Chumak, and B. Hillebrands, "Study of material parameters of YIG films with ferromagnetic resonance techniques", AG Magnetismus TU Kaiserslautern.